The common active site of Class I chelatases

Nathan Adams[1]

[1]University of Sheffield

July 24, 2017

Nathan B. P. Adams

Claudine Bisson,

Dimitris Ladakis

Amanda A. Brindley,

Evelyn Deery

Martin J Warren

C Neil Hunter

Abstract

Introduction

The central atom of any modified tetrapyrrole, either cobalt for cobalamin, iron for heme, nickel for F_{430} or magnesium for chlorophyll, is not only the key component of challenging reactions but its insertion into a modified tetrapyrrole can also a regulatory event and/or a branch point between the different biosynthetic pathways.

Magnesium chelatase (MgCH; E.C.6.6.1.1) catalyses the first committed step in chlorophyll biosynthesis, the insertion of a Mg^{2+} ion into protoporphyin IX. The MgCH complex consists of three obligate discrete subunits, identified in bacteriochlorophyll/chlorophyll producing organisms as BchI/ChlI (˜ 35 kDa), BchD/ChlD (˜ 75 kDa) and BchH/ChlH (˜150 kDa). In cyanobacteria and higher plants, a fourth subunit, Gun4, is required for full activity.(Davison et al., 2005; Mochizuki et al., 2001) Although the genes for MgCH were originally identified and recombinant protein expressed some time ago(Jensen et al., 1996), and extensive kinetic characterisation of the complex has identified the roles of the subunits(Reid and Hunter, 2004; Adams and Reid, 2013; Adams et al., 2014), the lack of structural information on the chelatase has hampered understanding the mechanism of this globally important protein.

In the aerobic biosynthesis of vitamin B12 (cobalamin) a cobalt ion is inserted into hydrogenobyrinic acid *a*,*c*-diamide (HBAD) by Cobalto chelatase (CoCH; E.C.6.6.2). Like MgCH, CoCH also consists of three subunits, superficially analogous to the MgCH subunits, designated CobS (˜ 36 kDa), CobT (˜70 kDa) and CobN (˜ 140 kDa), CobT (Scheme 1).

The BchI/ChlI, BchD/ChlD, CobT and CobS proteins are members of the ATPases associated with various cellular activities (AAA^+) super family of enzymes.(Gibson et al., 1995; Lundqvist et al., 2009) The low molecular weight I and S subunits larger D and S subunits share approximately 14 % sequence identity. The H and N subunits are the porphyrin binding subunits and share 22 % sequence identity. **BUT LATER WE SEE THEY SHARE LOADS OF STRUCTURAL SIMILARITY** CobN and ChlH share approximately 23 % sequence identity (figure XX).(Larkin et al., 2007)

The two AAA^+ subunits of each chelatase proteins form a complex(Jensen et al., 1996; Lundqvist et al., 2009, 2010; Fodje et al., 2001; Jensen et al., 1999) (either B/ChlID or CobST) which hydrolyses $MgATP^{2-}$ via an E.Pi complex(Adams and Reid, 2012), and the energy from hydrolysis used to power the metal ion insertion in the porphyrin binding subunit via an unknown mechanism. In MgCH, the ChlI protein is the active ATPase[11], whereas the ChlD protein appears to act as an allosteric control subunit, titrating the proteins response to Mg^{2+}.(Adams and Reid, 2013; Brindley et al., 2015) MgCH has been extensively characterised kinetically.(Brindley et al., 2015; Viney et al., 2007; Adams et al., 2016) The ChlI and ChlD proteins form a complex in an ATP dependent manner.(Adams and Reid, 2013; Jensen et al., 1999; GIBSON et al., 1999) This ChlID complex then appears to bind to ChlH via an unknown mechanism to receive the energy. ChlH is the site of porphyin binding and the site of metal ion insertion. The CoCH complex is less well characterised, but CobS and CobT form a dual ringed homohexamer in a similar fashion to the bacteriochlorophyll MgCH enzymes BchI and BchD.(Lundqvist et al., 2009, 2010)

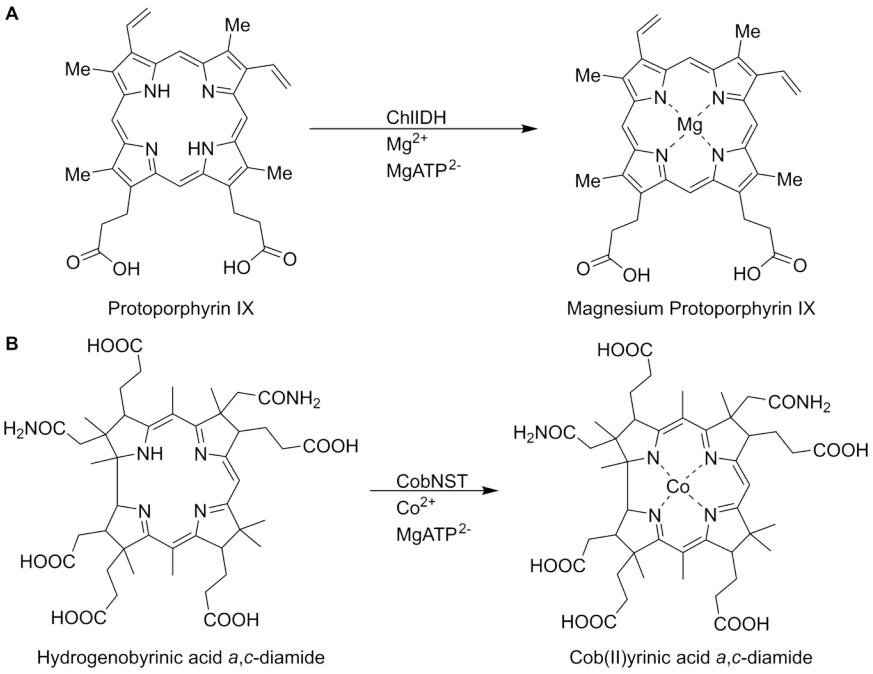

Figure 1: Couldn't find a caption, edit here to supply one.

Scheme 1. The reactions catalysed by (A) Magnesium chelatase (ChlIDH) and cobalto chelatase (CobNST)

MJW Group: CobNST historical background here.

In the case of cobalamin, cobalamin biosynthesis can occur via one of two distinct pathways, which are differentiated on the timing of the cobalt insertion into the macrocycle. A bacterium like *Salmonella enterica* will insert the cobalt at an early stage and before the ring gets contracted. It is often and not very accurately referred as the "anaerobic" pathway. This "early" cobalt insertion is performed by Class II type of chelatases, which do not require energy, including $CbiX^S$ (*Archaeoglobus fulgidus*, *Methanosarcina barkeri*), $CbiX^L$ (*Bacillus megaterium*) and CbiK (*Salmonella enterica*). Class II chelatases also include the *Bacillus subtilis* HemH and *B. megaterium* SirB, which insert iron into protoporphyrin IX (Haem pathway) or sirohydrochlorin (sirohaem pathway) respectively [Brindley et al 2003, JBC].

The alternative "aerobic" cobalamin biosynthetic pathway can be found in α-proteobacteria (including *Pseudomonas denitrificans, Brucella melitensis and Rhodobacter capsulatus*) where cobalt insertion occurs at a

much later stage, after the ring contraction and is highly dependent energetically. In *P. denitrificans*, either hydrogenobyrinic acid (HBA) or hydrogenobyrinic acid *a,c*-diamide (HBAD) can both act as substrate for the cobaltochelatase, the real substrate of the reaction was HBAD. Even if HBA was a poorer substrate with a K_{m} of 1.67 ± 0.17 μM in contrast to 0.085 ± 0.015 μM for HBAD, the real evidence came from the fact that not only cobyrinic acid was never detected in the cells but also *cobB* mutant (reaction responsible for the *a,c* side chain amidation) accumulated HBA and not cobyrinic acid (Figure 1) [Debussche et al 1990 +1992, Jbact]. This cobaltochelatase is part of the Class I chelatases, which also includes the magnesium chelatase (chlorophyll biosynthesis). This type of chelatase is composed of three proteins forming two separate subunits. The main subunit is a large monomeric protein, which binds the modified tetrapyrrole and is thought to be the catalytic component of the enzyme. The second subunit is an AAA^{+} (ATPases Associated with a variety of cellular Activities) chaperone-like complex, which can hydrolyse ATP. It is a complex structure of 2 proteins forming 2 polymonomeric rings on the top of each other. It is thought that ATP hydrolysis could involve conformational changes to the ATPases itself or in other molecules with which they interact, in this case the main monomeric subunit.

Historically the chelatase subunits have been resistant to crystallisation which has hampered efforts to obtain high resolution structural information. We previously published the low resolution (˜30 Å) negative stain apo-ChlH and ChlH-D_{IX} bound structures from *Thermosynechococcus elongatus* (Thermo) as determined by negative stain EM.[18] This structure revealed a two domain, with a small ˜ 16 kDa 'head' region and larger ±130 kDa body region which appeared to contain a cavity to hold the porphyrin substrate. Removal of N-terminal 'head' region of ChlH maintained some chelatase activity, confirming that the cavity region was the site of porphyrin binding. The atomic resolution structure of ChlH was only recently solved[19] which agreed with the previously published low resolution negative stain electron microscopy structures, but provided little in the way of further mechanistic understanding of the protein.

Here we show the crystal structures of N-terminal truncations of apo-CobN and CobN-HBAD which have a remarkably high degree of secondary and tertiary structural homology with a similar N-terminal truncation with ChlH and align with structure of the full protein. In addition via site directed mutagensis we describe two vital glutamic acids required for protein activity.

Experimental Methods

methods

MJW GROUP: CobN cloning method.

The cobS, cobT, cobN and cobB genes were amplified by PCR using genomic DNA from Brucella melitensis 16M (Bmei) and Rhodobacter capsulatus SB1003 (Rc) as templates. CobN genes were amplified with primers containing an AseI at the 5'end and SpeI and BamHI sites at the 3' end. Genes were cloned into pET14b into the NdeI and BamHI restriction sites. The cobS, cobT and cobB genes were amplified with primers containing a NdeI at the 5'end and SpeI and BamHI site at the 3' end. Genes were cloned into pET14b and pET3a into the NdeI and BamHI restriction sites. For co-expression of CobS and CobT, the corresponding genes were cloned consecutively, one from a pET14b construct keeping the fused poly-histidine tag leading sequence, and the second one from pET3a vector using the link and lock method (Raux al. 2009, in prep). Briefly, cobT was cut from pET3a using XbaI and BamHI and cloned into pET14b-cobS in 3' of the cobS into the SpeI and BamHI sites. This cloning generated the plasmid pET-cobSH-cobT. To construct the plasmid pET-cobS-cobTH, cobT was cut from pET14b using XbaI and BamHI and cloned into pET3a-CobS behind the cobS into the SpeI and BamHI sites of the pET vector.

Hydrogenobyrinic acid (HBA) and Hydrogenobyrinic acid a,c-diamide (HBAD) plasmids

The 9 or 10 genes required to synthesise HBA/HBAD in E. coli were cloned individually into pET3a after PCR. The different genes from the pET3a plasmids were assembled together following the link and lock method, as described above for the cobS and cobT co-expression vector. The pET3a-HBA plasmid contains the R. capsulatus cobA, cobI, cobJ, cobF, cobM, cobK, cobL, cobH as well as the B. melitensis cobG genes

in the following order: AIGJFMKLH. The pET3a-HBAD plasmids also contains the B. melitensis cobB.

Hydrogenobyrinic acid (HBA) production and purification

The HBA producing E. coli strain was grown in 2YT supplemented with 1 g/l of NH4Cl and antibiotics at 28°C for 24 hours. Cells were spun down, resuspended in 20 mM Tris HCl pH 7.5 and boiled for 10 minutes. The supernatant was applied to a diethylaminoethyl cellulose (DEAE)-Sephacel column. The column was washed with 100 mM and 200mM NaCl and the pink HBA was finally eluted with 300 mM NaCl. HBA was then further purified by passing through a LiChroprep RP18 column (Merck Chemicals) and eluted in ethanol.

Conversion of HBA to Hydrogenobyrinic acid a,c-diamide (HBAD)

The recombinant E. coli producing HBAD contains all the genes required to make HBA with both B. melitensis and R. capsulatus cobB. Despite having two copies of cobB, the bacteria were still producing a mixture of HBA and HBAD. Due to the poor turn over of the CobBs, an in vitro approach was developed to obtain pure HBAD from HBA. A recombinant E. coli, containing the pET3a-B. melitensis cobB and pLysS-R. capsulatus cobB, was used and both cobB were coexpressed. The cell lysate of the double cobB strain was mixed with HBA and incubated overnight at 25°C in 20 mM HEPES pH 7.5, 10 mM MgCl2, 5 mM ATP and 0.6 mg/l L-glutamine. The reaction mixture was applied to a DEAE-Sephacel column and the HBAD was isolated using an increasing gradient of NaCl. HBAD was finally eluted with 200 mM NaCl and further purified by high performance liquid chromatography (HPLC) using a reverse phase BDS Hypersil C-18 column (4.6 x 250 mm; Thermo Electron Corporation) on an Agilent 1100 series LC/MS Trap equipped with a diode array detector and eluted at a flow rate of 1 ml/min with a gradient of acetonitrile in 1 M ammonium acetate. The elution fractions were monitored at 328 nm and the HBAD containing fraction was collected.

AAB: SynH T_929 cloning method.

Protein Production/Purification Methods

MJW GROUP: CobN fragment xtalisation method please.

The SeMet incorporated construct representing the N-terminal third of *Thermococcal* ChlH (SeMet_T_929) (residues xxx – xxx) (10 mg ml^{-1} in buffer xxxxx) was crystallised by sitting drop vapour diffusion (xxx µl drop, 1:1 ratio, 1 ml reservoir) in xxxxx, xxxx and xxxx (drop C1 in T929 Semet plate at 10 mg/ml from 2/12/14) (290 K). Rough, cubic-shaped crystals formed after several days, which were harvested, cryoprotected in their mother liquor with an additional 25% ethylene glycol, and flash-cooled by plunging into liquid nitrogen. Data were collected on a single crystal at the selenium edge (λ= 0.97901 Å) on beamline i04 at the Diamond Light Source. The crystal belonged to the spacegroup $P2_1$ with cell dimensions of a=76.01 Å, b=139.81 Å, c=77.41 Å and β=108.63 °. Data were processed with Xia2 using a CC-half resolution cut-off of 1.93 Å. Shelx was used to locate ˜30 selenium sites that had an occupancy of >0.5 and build a poly-alanine starting model. This initial model was subjected to multiple rounds of manual model building in COOT and automated model building using Buccaneer, which resulted in a final model that contained four molecules of SeMet_T_929 within the asymmetric unit and a solvent content of 46 %. Refinement of this model using Refmac5 resulted in a final Rfactor of xxx and Rfree of xxx, with rmsds for bonds and angles of xx Å and xx °, respectively (See Table 1 for data collection and refinement statistics).

The full-length construct of wild-type ChlH from *Synechocystis sp.* (SynH) and a number of mutants (list mutants here) were crystallised by sitting-drop vapor diffusion (xxx µl drop, 1:1 ratio, 1 ml reservoir) in 0.8-1.2 M Sodium citrate pH 7.0 and 2 mM dithiothreitol (DDT) (290 K). Large triangular rod-shaped crystals grew within several days, which were cryoprotected in Paratone N oil and flash-cooled with liquid nitrogen. Data from wild-type protein crystals were collected to 2.54 Å resolution and were processed with Xia2. The crystals belonged to the spacegroup H3 with cell dimensions of a=b[?]320, c[?]105, α=β=90 °, γ=120 °. An initial model was determined directly by refinement in Refmac5 using PDB: XXXX (REF other synH paper). However, after several rounds of model building in COOT and further refinement, it became apparent that

a number of disordered loops were present in the structure. To aid in the interpretation of these loops, a set of experimental phases were also obtained by single wavelength anomalous diffraction from crystals of the wild-type enzyme that were soaked (3 hr) with Tantalum bromide (Ta_2Br_{16}), which was added directly to the drop as a solid. Four Ta_2Br_{16} clusters were located using AUTOSHARP, which enabled a more complete 3.0 Å resolution structure to be modelled *de novo* in Buccaneer. The crystals of the mutant enzyme belonged to the same spacegroup and cell dimensions as the wild-type protein, so the structures were determined directly by refinement at similar resolutions to the wild-type enzyme. In all cases difference density indicated the position of the mutated residue, which was modelled and refined to acceptable B factors (See table 1 for data collection and refinement statistics).

Magnesium chelatase assays

Assays were performed in 50 mM MOPS/KOH, 0.3 M glycerol, I = 0.1 (KCl) at 34 °C with substrate concentrations of 15 mM $MgCl_2$, 5 mM ATP, 8 µM $D_{IX,}$ unless otherwise stated in figure legends. Assays were initiated by the addition of enzyme to give final concentrations of 0.1 mM ChlD, mM 0.2 mM ChlI and 0.4 mM ChlH. Steady state assays of magnesium chelatase followed formation of the product, MgDIX, over a period of one to two hours. Reaction progress was monitored using a Omega FluoStar microplate reader (BMG LabTech, Aylesbury, UK), with excitation at 420 ± 5 nm and emission detected at 580 ± 5 nm. Steady state rates (v_{ss}) were calculated using software supplied by the manufacturer (MARS version 2.41). Non-linear regression analysis was performed using Igor Pro (v. 7.0.1).

Results

Structure of CobN fragment bound to HBAD

MJW GROUP SECTION with CB

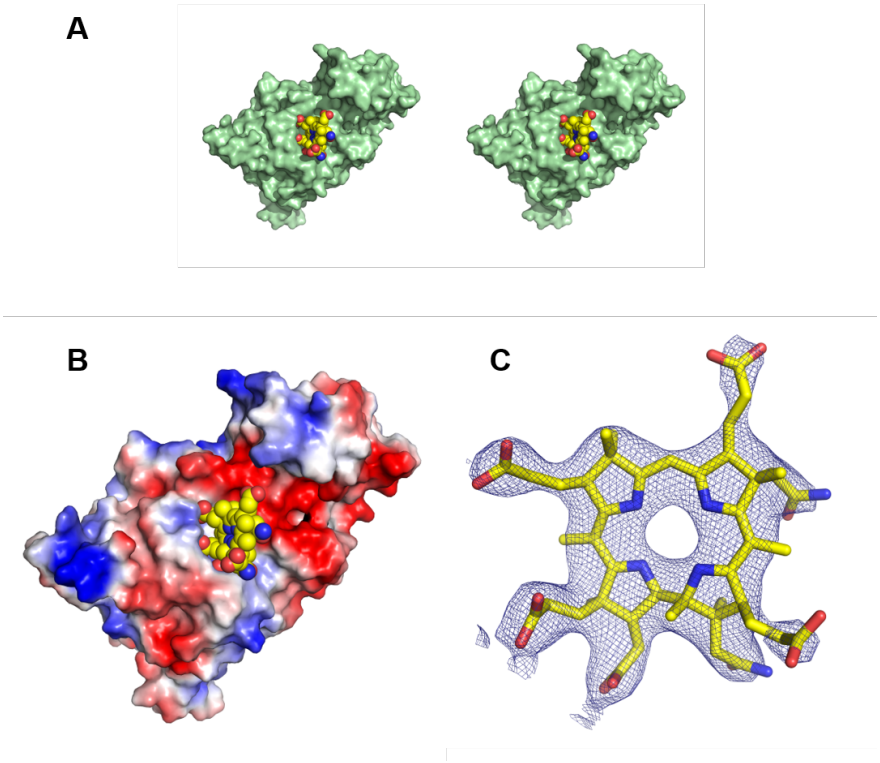

Abbildung 2: Couldn't find a caption, edit here to supply one.

Figure 1. (A) A stereo diagram showing a surface representation of the C-terminal fragment of CobN (T_865) (green) in complex with HBAD (yellow carbon atoms), which sits within a shallow pocket on the surface of the protein. In (B) the protein is shown in the same view and the electrostatic surface has been calculated (Pymol) surrounding the HBAD binding site. Red represents negative charge, white is neutral and blue represents positive charge. (C) shows the quality of the 2Fo-Fc map (black mesh, contoured at 1 σ) surrounding HBAD in the T_865 complex.

Crystal structure of the T_929 fragment of ChlH

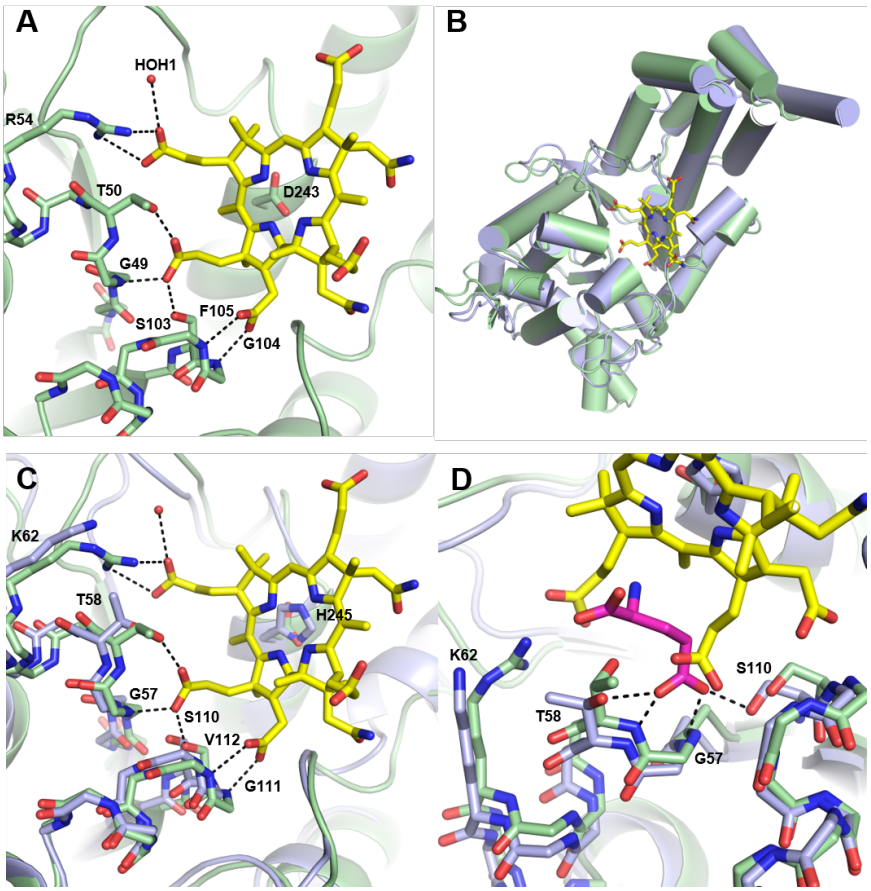

Figure 3: Couldn't find a caption, edit here to supply one.

Figure 2. (A) Details of the interactions made between HBAD (yellow carbon atoms) and the N-terminal fragment of CobN (T_865) (green carbon atoms). The protein backbone is drawn as a cartoon, with important side chains and the HBAD drawn as sticks and coloured with atom colours (O=red, N=blue). Hydrogen bond interactions between the HBAD and the protein are represented by dashed black lines. The water molecule (HOH1) is drawn as a small red sphere. In (B) the CXXX/HBAD complex is superimposed onto the equivalent construct of *Thermococcal* H subunit (T_929) (blue) (RMSD=X.X). The mainchain is drawn as a cartoon, with helices represented at cylinders. HBAD is represented as in part A. (C) shows the conservation of residue charge and position within the porphyrin binding pocket of C_XXX and T_929. However, D243, which sits behind the tetrapyrole ring in C_XXX is exchanged for a histidine in T_929 (H245), reflecting a change in charge within this region of the binding pocket. (D) shows the binding position of a likely carboxyl group of an unknown

ligand (magenta carbon atoms, modelled with a GLU) in complex with T_929 (See Figure S2 for electron density map). Each carboxyl oxygen forms two hydrogen bonds, one with the main chain and one with either T58 or S110, exploiting the positive dipole created by the helix which sits below it.

Identification of Porphyrin Binding site in ChlH

CB to describe modelling

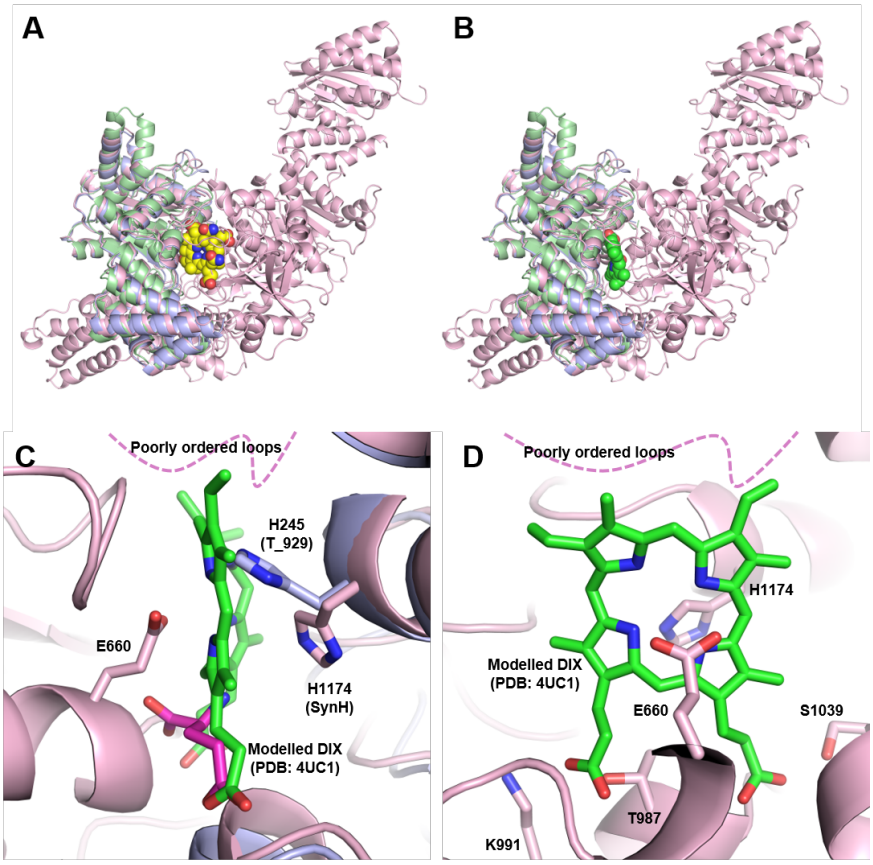

Figure 4: Couldn't find a caption, edit here to supply one.

Figure 3. In (A) SynH (pink), T_929 (blue) and C_XXX (green) are superimposed, with the protein backbone drawn as a cartoon. HBAD is drawn as spheres with yellow carbon atoms to show the position of the putative active site in SynH. In (B) the view is the same, but HBAD is replaced with a modelled position of DIX (spheres, green carbons) showing a rotation of the porphyrin ring in the putative active site. The modeling of DIX is based on the position of the carboxyl group of the unknown ligand in the T_929 complex (magenta carbon atoms), shown in (C). The conformation of DIX is slightly bent (PDB: 4UC1), which fits comfortably within the putative active site of SynH and indicates the position of a pair of residues (E660 and H1174) within the binding pocket that flank either side of magnesium site at the centre of the porphyrin ring. In (D) the view of the putative active site is rotated by 90° and the position of the residues that interact with the DIX are shown as sticks.

Figure XX: **A**, Potential residues that stabilise or destabilise porphyrin binding. Full length ChlH represented as grey cartoon, T929 truncation as purple cartoon. Important residues in ChlH represented as lines and

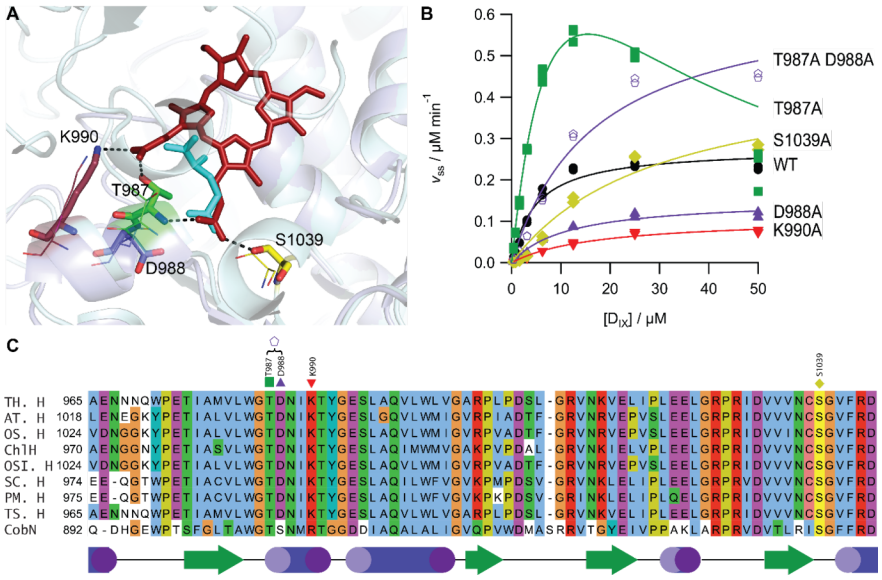

Figure 5: Couldn't find a caption, edit here to supply one.

corresponding residues in T929 represented as sticks and coloured as in **B.** D_{IX} is represented as sticks in red and has been modelled into the active site in a similar location as the 'mysterious' ligand that is present in the crystal structure in T929**. B,** Steady state magnesium chelatase assays with respect to [D_{IX}]. Assays contained 0.1 μM ChlD, 0.2 μM ChlI, 0.4 μM ChlH WT or mutant in 50 mM MOPS/KOH, 0.3 M glycerol, 1 mM DTT, 10 mM free Mg^{2+}, 5 mm $MgATP^{2-}$. Steady state rates were fitted to the Michaelis-Menten equation (equation X) except T987A where the line is fitted to a substrate inhibition equation, but gives physiologically impossible fit coefficients. Fit coefficients are listed in table X1. **C**, Extract of sequence alignment and seconday structure representation of the sequence highlighting the level of conservation amongst ChlH proteins and CobN for these core residues.

Protein	K_{cat} / min^{-1}	K_M / μM	K_{cat}/K_μ / $\mu\nu^{-1}$ μM^{-1}
WT	0.69 ± 0.03	4.8 ± 0.8	0.14 ± 0.02
D988A	0.38 ± 0.02	11.4 ± 1.9	0.03 ± 0.01
K990A	0.27 ± 0.02	17.2 ± 2.7	0.02 ± 0.01
S1039A	1.19 ± 0.17	29.9 ± 8.4	0.04 ± 0.01
T987A D988A	1.63 ± 0.14	16.9 ± 3.3	0.10 ± 0.02

E660 is vital for protein activity

E660 was deemed a likely candidate to mediate Mg^{2+} ion insertion into the porphyrin ring. Based on molecular modelling (figure 3) and multiple sequence alignments (figure XX B). Mutation of the residue to an acidic but shorter aspartic acid reduced activity by 95 or neutral side chain.

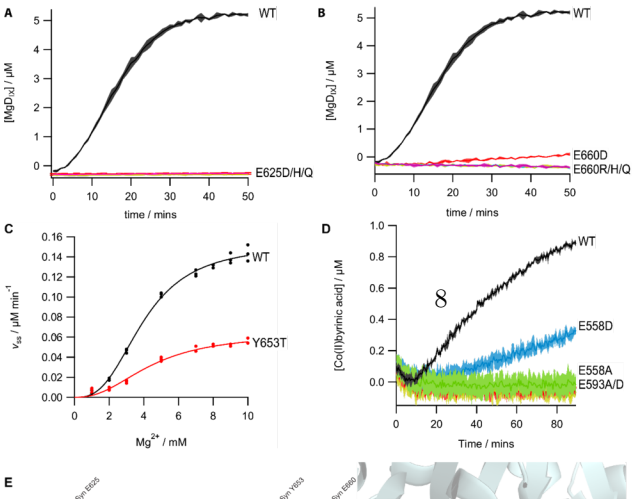

περφορμεδ ιν τριπλιςατε ανδ δισπλαψεδ ας μεαν ωιτη στανδ δειατιον σηοων ιν σηαδινγ. ˜, **E625 ανδ E660 αρε ςονσερεδ τηρουγηουτ τηε οβσερεδ ήλH** προτεινς ααιλαβλε (τοπ αλιγνμεντ, σεε συππλεμενταρψ φιγυρε ΞΞ φορ φυλλ αλιγνμεντ) ανδ βετωεεν ήλH ανδ ὸβN (βοττομ αλιγνμεντ, σεε συππλεμενταρψ φιγυρε ΞΞ φορ φυλλ αλιγνμεντ).

Protein	Protein	V_{ss} / μM min^{-1}	v_{rel}
ChlH	WT	0.230 ± 0.009	1
ChlH	E625D	n.d.	0
ChlH	E625H	n.d.	0
ChlH	E625Q	n.d.	0
ChlH	E660R	n.d.	0
ChlH	E660H	n.d.	0
ChlH	E660Q	n.d.	0
ChlH	E660D	0.012 ± 0.001	0.05
CobN	WT	0.016 ± 0.001	1
CobN	E558A	n.d.	0
CobN	E558D	0.003 ± 0.001	0.19
CobN	E593A	n.d.	0
CobN	E593D	n.d.	0

Table 1: The maximal and relative rates of ChlH WT, E625 and E660, CobN WT, E558 and E593A mutants calculated as the mean maximum slope of the curve over ten minutes errors one standard deviation.

H1174V and Asp 1101 are not required.

PD, JV work from ages ago and my repeats found the H1074 in SynH, even though it is in the active site is not involved in catalysis (no difference in activity). Mo found a reference in an MJW document that mutating the structurally analogous D1101 also has no effect on activity..

Discussion/Conclusions

Extra Figures:

Alignment **H and N**

P73020 P73020_SYNY3 1MFTNVKSTIRRVDPEALNGRQLLKVVYVVLESQYQSALSAAVRNINRTNSS-LAIQLTGYL 60

O53498 O53498_MYCTU 1----------MPEPTVLLLSTS----------DTDL 16

P73020 P73020_SYNY3 61IEELRDPENYANFKHDVSEANLFIASLIFIEDLADKVVEAVTPYRDNLDAAIVF-PSMPQV 120

O53498 O53498_MYCTU 17ISARSSGKNYRW-ANPSRLSDLELTDL-----LA----------EASI 48

P73020 P73020_SYNY3 121MRLNKMGSFSMAQLGQSKSAIAQFMKKRKENSSGAGFQDAMLKLLRTLPTVLKY----- 174

O53498 O53498_MYCTU 49VVIRILGGYRAWQSGIDT-----V----------IAGGVPAVLVSGEQAAD 84

P73020 P73020_SYNY3 175--LPVEKAQDARNFMLSFQYWLGGSQENLENFLLMLTDKYVYPDLGLDKLVNYQEPVVY

O53498 O53498_MYCTU 85AELTDRSTVAAGTALQAHIYLAHGGVDNLRELHAFLCDTVLMTGFG----FTPPVATP 138

P73020 P73020_SYNY3 233DMGIWHPLSMQMFENVKDYLEWYNQRPDISEDLKDPLAPCIGLIMQRTH-LVTGDDAHYVG 292

O53498 O53498_MYCTU 139TWGVLE----------RPDA-----GKTGPTIAVLYYRAQHLAGNTGYVEA 174

P73020 P73020_SYNY3 293MVQELEAMGARVICVFSGGLDFSKPVNEYFWDKSVNGVEPLPIVDAVVSLTGFALV-GGP 351

O53498 O53498_MYCTU 175LCRAIEDAGGRPLPLYCASLRTAEPRLL----ERLGGADAM--VVTVLAAGGVKPAAASA 2

P73020 P73020_SYNY3 352ARQDHPRAIESLKKLNRPYMCALPLVFQTTEEWEASDLGLHPIQVALQI-AIPELDGAIEP 411

O53498 O53498_MYCTU 229GGDDDSWNVEHLAALDIPILQGLC-LTSPRDQWCANDDGLSPLDVASQVAVPEFDGRIIT

P73020 P73020_SYNY3 412IILSGRDGSTGRAI---ALQDRLEAIAQRAMKWANLRKKPKLDKKVAITVFSFPPDKGNV 4

O53498 O53498_MYCTU 288VPFSFKEIDDDGLISYVADPERCARVAGLAVRHARLRQVAPADKRVALVF-SAYPTKHARI 347

P73020 P73020_SYNY3 469GTAAYLDVFGSIYEVMKGLQGNGYDVQDLPGSAKELMEAVIHDAQAQY-NSPEL------ 521

O53498 O53498_MYCTU 348GNAVGLDTPASAVALLQAMRQRGYRVGDLPGVESNDGDALIHALIECG-GHDPDWLTEGQL 407

P73020 P73020_SYNY3 522-NIAHRMSVEQYERL-----TPYSVRLEENWGKPPGHLNSDG-----QNLLIYGKEFGNV 570

O53498 O53498_MYCTU 408AGNPIRVSAKEYRDWFATLPAELTDVVTAYWGPPPGELFVDRSHDPDGEIVI-AALRAGNL 467

P73020 P73020_SYNY3 571FIGVQPTFGYEGDPMRLLFSRSASPHHGFAAYYTYLNH----IWKADAVLHFGTHGSLEF 62

O53498 O53498_MYCTU 468VLMVQPPRGFGENPVAIYHDPDLPPSHHYLAAYRWLDTGFSNGFGA-HAVVHLGKHGNLEW 527

P73020 P73020_SYNY3 627MPGKQMGMSGECYPDNLIGTIPNLYYYAANNPSEATIAKRRGYASTISYLTP-PAENAGLY 686

O53498 O53498_MYCTU 528LPGKTLGMSASCGPDAALGDLPLIYPFLVNDPGEGTQAKRRAHAVLVDHLIPP-MARAETY 587

P73020 P73020_SYNY3 687KGLQELNELIGSYQTLKD--SGRGIQIVNTIMDQARICNLDQDVNLPDINAEEMDQGQRD 7

O53498 O53498_MYCTU 588GDIARLEQLLDEHASVAALDPGKLPAIRQQIWTLIRAAKMDHDLGLTERPEE---DSFD 643

P73020 P73020_SYNY3 745TIVGSVYRKLMEIESRLLPCGLHVIGQPPSAEEAIATLVNIASLDREDEGI-WALPTLIAE 804

O53498 O53498_MYCTU 644DMLLHVDGWLCEIKDVQIRDGLHILGQNPTGEQELDLVLAILRARQLFG-GAHAIPGLRQA 703

P73020 P73020_SYNY3 805SIGRNMEEIYRNSDKGILADVELLQDITLATRAAVAALVQEQINADGRVS-FVSKLNFFKI 864

O53498 O53498_MYCTU 704-LGLAE--------DGTDERAT-VDQTEAKARELVAA---------- 730

P73020 P73020_SYNY3 865GKKAPWVKSLCDSGYPNVNEEKLKPLFEYLEFCLEQVCADNEFGGLLQALEGEYVLPGI

O53498 O53498_MYCTU 731LQATGWDPSAADRLTGNADAAA-VLRFAATEVIPRLAGTATEIEQVLRALDGRFIPAGPS

P73020 P73020_SYNY3 925GDPIRN-PNVLPTGKNIHALDPQSIPTLAAVQSAKVVVDRLLERQRAENGGNYPETIASV

O53498 O53498_MYCTU 790GSPLRGLVNVLPTGRNFYSVDPKAVPSRLAWEAGVALADSLLARYRDE-HGRWPRSVGLS 848

P73020 P73020_SYNY3 984LWGTDNIKTYGESLAQIMWMVGAKPVPDALG-RVNKIELVPLEELGRPRIDVVVNCSGVF

O53498 O53498_MYCTU 849VWGTSAMRTAGDDIAEVLALLGVRPVWDDASRRVIDLAPMQPAEL-GRPRIDVTVRISGFF 908

P73020 P73020_SYNY3 1043RDLFINQMNLLDQAVKLAAEADEPLEMNFVRKHALEQAEEMGIGVREAA-TRIFSNASGSY 1102

O53498 O53498_MYCTU 909RDAFPHVVTMLDDAVRLVADLDEAAEDNYVRAHAQADLAHHG-DQRRATTRIFGSKPC

P73020 P73020_SYNY3 1103SSNVNLAVENSSWEDESELQEMYLKRKSFAFNSDNPGMMDQNRDMFER-ALKTADATFQNL 1162

O53498 O53498_MYCTU 968GAGLLQLIDSRSWRDDADLAQVYTAWGGFAYGRDLDGREAI--DDMNRQYRRIAVAAKN

P73020 P73020_SYNY3 1163DSSEISLTDVSHYFDSDPTKLISTLRDDGKAPAAYIADTTTANA-QVRTLSETVRLDART 1

O53498 O53498_MYCTU 1026DTREHDIADSDDYFQYHGGMVATVRALTGQAPAAYIGDNTRPDAIRTRTLSEET-TRVFRA 1085

P73020 P73020_SYNY3 1222KLLNPKWYEGMLSHGYEGVRELSKRLVNTMGWSATAGAVDNWVYEDANST-FIKDEEMCKR 1281

O53498 O53498_MYCTU 1086RVVNPRWMAAMRRHGYKGAFEMAATVDYLFGYDATAGVMADWMYE-QLTQRYVLDAQNRTF 1145

P73020 P73020_SYNY3 1282LMDLNPNSFRRMVSTLLEVNGRGYWETSD-ENLERLQELYQEVEDRIEGVE 1331

O53498 O53498_MYCTU 1146MTESNPWALHGMAERLLEAAGRGLWAQPAPETLDGLRQVLLETEGDLEA-- 1194

ate of job execution	Jun 1, 2017
Job identifier	A201706018A530B6CA0138AFAA6D2B97CE8C2A924D333685 (jobs are stored for 7 days)
Running time	14.4 seconds
Identical positions	341
Identity	24.872%
Similar positions	401
Program	clustalo
Default parameters	Default parameters: The default transition matrix is Gonnet, gap opening penalty is 6 bits, gap exte

1

1. Davison, P. A. *et al.* Structural and biochemical characterization of Gun4 suggests a mechanism for its role in chlorophyll biosynthesis. *Biochemistry* **44,** 7603–12 (2005).

2. Mochizuki, N., Brusslan, J. a, Larkin, R., Nagatani, a & Chory, J. Arabidopsis genomes uncoupled 5 (GUN5) mutant reveals the involvement of Mg-chelatase H subunit in plastid-to-nucleus signal transduction. *Proc. Natl. Acad. Sci. U. S. A.* **98,** 2053–8 (2001).

3. Jensen, P. E., Gibson, L. C., Henningsen, K. W. & Hunter, C. N. Expression of the chlI, chlD, and chlH genes from the Cyanobacterium synechocystis PCC6803 in Escherichia coli and demonstration that the three cognate proteins are required for magnesium-protoporphyrin chelatase activity. *J. Biol. Chem.* **271,** 16662–16667 (1996).

4. Reid, J. D. & Hunter, C. N. Magnesium-dependent ATPase activity and cooperativity of magnesium

chelatase from Synechocystis sp. PCC6803. *J. Biol. Chem.* **279,** 26893 (2004).

5. Adams, N. B. P. & Reid, J. D. The Allosteric Role of the AAA+ Domain of ChlD Protein from the Magnesium Chelatase of Synechocystis Species PCC 6803. *J. Biol. Chem.* **288,** 28727–28732 (2013).

6. Adams, N. B. P., Marklew, C. J., Brindley, A. A., Hunter, C. N. & Reid, J. D. Characterization of the magnesium chelatase from Thermosynechococcus elongatus. *Biochem. J.* **457,** 163–70 (2014).

7. Gibson, L. C., Willows, R. D., Kannangara, C. G., von Wettstein, D. sphaeroides: reconstitution of activity by combining the products of the bchH, -I, and -D genes expressed in Escherichia coli. *Proc. Natl. Acad. Sci. U. S. A.* **92,** 1941–4 (1995).

8. Lundqvist, J. *et al.* The AAA(+) motor complex of subunits CobS and CobT of cobaltochelatase visualized by single particle electron microscopy. *J. Struct. Biol.* **167,** 227–34 (2009).

9. Larkin, M. a *et al.* Clustal W and Clustal X version 2.0. *Bioinformatics* **23,** 2947–8 (2007).

10. Fodje, M. N. *et al.* Interplay between an AAA module and an integrin I domain may regulate the function of magnesium chelatase. *J. Mol. Biol.* **311,** 111–22 (2001).

11. Jensen, P. E., Gibson, L. & Hunter, C. N. ATPase activity associated with the magnesium-protoporphyrin IX chelatase enzyme of Synechocystis PCC6803: evidence for ATP hydrolysis during Mg2+ insertion, and the MgATP-dependent interaction of the ChlI and ChlD subunits. *Biochem. J.* **339,** 127 (1999).

12. Adams, N. B. P. & Reid, J. D. Nonequilibrium isotope exchange reveals a catalytically significant enzyme-phosphate complex in the ATP hydrolysis pathway of the AAA+ ATPase magnesium chelatase. *Biochemistry* **51,** 2029–2031 (2012).

13. Brindley, A. A., Adams, N. B. P., Hunter, C. N. & Reid, J. D. Five Glutamic Acid Residues in the C-Terminal Domain of the ChlD Subunit Play a Major Role in Conferring Mg 2+ Cooperativity upon Magnesium Chelatase. *Biochemistry* **54,** 6659–6662 (2015).

14. Viney, J., Davison, P. A., Hunter, C. N. & Reid, J. D. Direct measurement of metal-ion chelation in the active site of the AAA+ ATPase magnesium chelatase. *Biochemistry* **46,** 12788–94 (2007).

15. Adams, N. B. P., Brindley, A. A., Hunter, C. N. & Reid, J. D. The catalytic power of magnesium chelatase: a benchmark for the AAA+ ATPases. *FEBS Lett.* **590,** 1687–1693 (2016).

16. Gibson, L., Jensen, P. E. & Hunter, C. N. Magnesium chelatase from Rhodobacter sphaeroides: initial characterization of the enzyme using purified subunits and evidence for a BchI-BchD complex. *Biochem. J.* **337,** 243 (1999).

17. Lundqvist, J. *et al.* ATP-induced conformational dynamics in the AAA+ motor unit of magnesium chelatase. *Structure* **18,** 354–365 (2010).

18. Qian, P. *et al.* Structure of the Cyanobacterial Magnesium Chelatase H Subunit Determined by Single Particle Reconstruction and Small-angle X-ray Scattering. *J. Biol. Chem.* **287,** 4946–4956 (2012).

19. Chen, X. *et al.* Crystal structure of the catalytic subunit of magnesium chelatase. *Nat.Plants* (2015).

References

Nathan B. P. Adams and James D. Reid. Nonequilibrium Isotope Exchange Reveals a Catalytically Significant Enzyme–Phosphate Complex in the ATP Hydrolysis Pathway of the AAA+ATPase Magnesium Chelatase. *Biochemistry*, 51(10):2029–2031, mar 2012. doi: 10.1021/bi300149z. URL https://doi.org/10.1021%2Fbi300149z.

Nathan B P Adams and James D Reid. The Allosteric Role of the AAA+ Domain of ChlD Protein from the Magnesium Chelatase of Synechocystis Species PCC 6803. *Journal of Biological Chemistry*, 288: 28727–28732, 2013. doi: 10.1074/jbc.M113.477943.

Nathan B P Adams, C.J. Marklew, P. Qian, A.A. Brindley, P.A. Davison, P.A. Bullough, and C.N. Hunter. Structural and functional consequences of removing the N-terminal domain from the magnesium chelatase ChlH subunit of Thermosynechococcus elongatus. *Biochemical Journal*, 464(3):315–322, 12 2014. ISSN 14708728 02646021. doi: 10.1042/BJ20140463. URL http://www.pubmedcentral.nih.gov/articlerender.fcgi?artid=4255732&tool=pmcentrez&rendertype=abstracthttp://www.ncbi.nlm.nih.gov/pubmed/25471602.

Nathan B. P. Adams, Amanda A. Brindley, C. Neil Hunter, and James D. Reid. The catalytic power of magnesium chelatase: a benchmark for the AAA+ATPases. *FEBS Letters*, 590(12):1687–1693, jun 2016. doi: 10.1002/1873-3468.12214. URL https://doi.org/10.1002%2F1873-3468.12214.

Amanda A. Brindley, Nathan B. P. Adams, C. Neil Hunter, and James D. Reid. Five Glutamic Acid Residues in the C-Terminal Domain of the ChlD Subunit Play a Major Role in Conferring Mg 2+ Cooperativity upon Magnesium Chelatase. *Biochemistry*, 54(44):6659–6662, 11 2015. ISSN 0006-2960. doi: 10.1021/acs.biochem.5b01080. URL http://pubs.acs.org/doi/10.1021/acs.biochem.5b01080http://www.ncbi.nlm.nih.gov/pubmed/26513685.

Paul A Davison, Heidi L Schubert, James D Reid, Charles D Iorg, Annie Heroux, Christopher P Hill, and C Neil Hunter. Structural and biochemical characterization of Gun4 suggests a mechanism for its role in chlorophyll biosynthesis. *Biochemistry*, 44(21):7603–12, 5 2005. ISSN 0006-2960. doi: 10.1021/bi050240x. URL http://www.ncbi.nlm.nih.gov/pubmed/15909975.

M N Fodje, A Hansson, M Hansson, J G Olsen, S Gough, R D Willows, and S Al-Karadaghi. Interplay between an AAA module and an integrin I domain may regulate the function of magnesium chelatase. *Journal of molecular biology*, 311(1):111–22, 8 2001. ISSN 0022-2836. doi: 10.1006/jmbi.2001.4834. URL http://www.ncbi.nlm.nih.gov/pubmed/11469861.

L C Gibson, R D Willows, C G Kannangara, D von Wettstein, and C N Hunter. Magnesium-protoporphyrin chelatase of Rhodobacter sphaeroides: reconstitution of activity by combining the products of the bchH, -I, and -D genes expressed in Escherichia coli. *Proceedings of the National Academy of Sciences of the United States of America*, 92(6):1941–4, 3 1995. ISSN 0027-8424. URL http://www.pubmedcentral.nih.gov/articlerender.fcgi?artid=42398&tool=pmcentrez&rendertype=abstract.

Lucien C.D. GIBSON, Poul Erik JENSEN, and C. Neil HUNTER. Magnesium chelatase from Rhodobacter sphaeroides: initial characterization of the enzyme using purified subunits and evidence for a BchIBchD complex. *Biochemical Journal*, 337(2):243, jan 1999. doi: 10.1042/0264-6021:3370243. URL https://doi.org/10.1042%2F0264-6021%3A3370243.

P E Jensen, L C Gibson, K W Henningsen, and C N Hunter. Expression of the chlI, chlD, and chlH genes from the Cyanobacterium synechocystis PCC6803 in Escherichia coli and demonstration that the three cognate proteins are required for magnesium-protoporphyrin chelatase activity. *The Journal of biological chemistry*, 271(28):16662–16667, 7 1996. ISSN 0021-9258. URL http://www.ncbi.nlm.nih.gov/pubmed/8663186.

P.E. Jensen, LC Gibson, and C.N. Hunter. ATPase activity associated with the magnesium-protoporphyrin IX chelatase enzyme of Synechocystis PCC6803: evidence for ATP hydrolysis during Mg2+ insertion, and the MgATP-dependent interaction of the ChlI and ChlD subunits. *Biochemical Journal*, 339(Pt 1):127, 1999. URL http://www.ncbi.nlm.nih.gov/pmc/articles/PMC1220136/.

M.A. Larkin, G. Blackshields, N.P. Brown, R. Chenna, P.A. McGettigan, H. McWilliam, F. Valentin, I.M. Wallace, A. Wilm, R. Lopez, J.D. Thompson, T.J. Gibson, and D.G. Higgins. Clustal W and Clustal X version 2.0. *Bioinformatics*, 23(21):2947–2948, sep 2007. doi: 10.1093/bioinformatics/btm404. URL https://doi.org/10.1093%2Fbioinformatics%2Fbtm404.

Joakim Lundqvist, Dominika Elmlund, Dana Heldt, Evelyne Deery, Christopher a G Söderberg, Mats Hansson, Martin Warren, and Salam Al-Karadaghi. The AAA(+) motor complex of subunits CobS and CobT of cobaltochelatase visualized by single particle electron microscopy. *Journal of structural biology*, 167(3):227–34, 9 2009. ISSN 1095-8657. doi: 10.1016/j.jsb.2009.06.013. URL http://www.ncbi.nlm.nih.gov/pubmed/19545636.

Joakim Lundqvist, Hans Elmlund, Ragna Peterson Wulff, Lisa Berglund, Dominika Elmlund, Cecilia Emanuelsson, Hans Hebert, Robert D Willows, Mats Hansson, Martin Lindahl, and Salam Al-Karadaghi. ATP-induced conformational dynamics in the AAA+ motor unit of magnesium chelatase. *Structure*, 18 (3):354–65, 3 2010. ISSN 1878-4186. doi: 10.1016/j.str.2010.01.001. URL http://www.ncbi.nlm.nih.gov/pubmed/20223218.

N Mochizuki, J a Brusslan, R Larkin, a Nagatani, and J Chory. Arabidopsis genomes uncoupled 5 (GUN5) mutant reveals the involvement of Mg-chelatase H subunit in plastid-to-nucleus signal transduction. *Proceedings of the National Academy of Sciences of the United States of America*, 98(4):2053–8, 2 2001. ISSN 0027-8424. doi: 10.1073/pnas.98.4.2053. URL http://www.pubmedcentral.nih.gov/articlerender.fcgi?artid=29380&tool=pmcentrez&rendertype=abstract.

J.D. Reid and C.N. Hunter. Magnesium-dependent ATPase activity and cooperativity of magnesium chelatase from Synechocystis sp. PCC6803. *Journal of Biological Chemistry*, 279(26):26893, 2004. ISSN 0021-9258. doi: 10.1074/jbc.M400958200. URL http://www.jbc.org/content/279/26/26893.short.

Joanne Viney, Paul A. Davison, C. Neil Hunter, and James D. Reid. Direct Measurement of Metal-Ion Chelation in the Active Site of the AAA+ATPase Magnesium Chelatase†. *Biochemistry*, 46(44):12788–12794, nov 2007. doi: 10.1021/bi701515y. URL https://doi.org/10.1021%2Fbi701515y.